

Preliminary Assessment of Millimeter Wave Plane Wave Generator For 5G Device Testing

F. Scatton¹, D. Sekuljica¹, A. Giacomini¹, F. Saccardi¹, A. Scannavini¹,
E. Kaverine², S. Anwar², N. Gross², P. O Iversen², L. J. Foged¹

¹ MVG, Microwave Vision Italy SRL, Pomezia, Italy, lars.foged@mvg-world.com

² MVG, Microwave Vision, Paris, France, nicolas.gross@mvg-world.com

Abstract—In this paper, early performance assessments on a newly developed plane wave generator (PWG) at millimeter wave frequencies are reported for the first time. The PWG is integrated in an automated system suitable for 5G testing. Far-field radiation from devices such as pattern, beam pointing, and typical over-the-air (OTA) parameters can be measured in 3D space. Devices are positioned in the quiet zone (QZ) using a RF transparent positioner. Live person testing is feasible, using a chair placed in the system such that the device including head and upper torso of the test person is within the QZ.

The PWG based system is described in this paper, including a preliminary evaluation of measurement performance and accuracy at system level. The assessment is based on system simulation, measurement post-processing, and actual test on a pilot system. The PWG technology discussed in this paper is currently being integrated as a standard product.

Index Terms—antenna measurements, plane wave generator.

I. INTRODUCTION

Since 5G standards at millimeter frequencies were approved, testing solutions have mainly been founded on direct far-field (FF). Device testing is performed over-the-air (OTA) to determine the antenna system performances without a direct connection to the device. For 3G/4G type devices it is often sufficient to determine total power-based parameters into and out of the device. For 5G devices there is a need to determine also patterns and pointing directions in 3D space. For electrically large devices like base-stations and user terminals, a sizable separation between the probe/range antenna and the device is required to achieve a good approximation to FF. The large separation leads to high free-space attenuation which can limit the dynamic range and impact the quality of the measured DUT parameters.

An alternative to direct FF measurements using a probe or range antennas is to use a Plane Wave Generator (PWG). Examples of such solutions are the Compact Antenna Test Range (CATR) and array based PWG [1-6]. The PWG approximate the FF plane wave in the test volume of the device at a close distance. Reciprocity ensure that both transmit and receive testing can be performed with sufficient accuracy. The shorter distance and PWG gain reduce the losses due to free space attenuation and decrease the overall system size.

Both array-based PWG and the CATR can be considered special cases of Near-Field (NF) techniques [2]. In NF measurements, a mathematical transformation is applied to derive the FF from the measured amplitude and phase data in the NF. In case of both CATR and PWG, the field transformation is implemented at the hardware level. The CATR perform the field sampling over a continuous surface of the reflector to derive the approximate FF. The PWG take advantage of the discrete sampling by array elements and perform the transformation from the NF samples to FF by way of a beam forming network (BFN) behind the array. Both the CATR and PWG are considered valid testing solutions by the standardization communities such as CTIA and 3GPP.

A dual polarized PWG covering the frequency range from 600MHz to 6GHz was presented in [3-4]. The development and technology validation of sub-components, essential to the development of a full size PWG system at millimeter wave frequencies are presented in [7]. The frequency range of the millimeter wave PWG system, shown in Fig. 1 (left), is 24-30GHz, which includes 5G FR2 bands 257, 258 and 261. Measurement capabilities in 3D are achieved by rotating the PWG in elevation while the device under test is rotated in azimuth. The system is designed with a spherical quiet zone (QZ) of diameter 350mm, at 1200mm from the PWG aperture.

In this paper, measurements, and simulations on a pilot system, shown in Fig. 1 (right), are used in a preliminary evaluation of measurement performance and accuracy for PWG based systems at millimeter wave frequencies.



Fig. 1. The 24-30GHz millimeter wave plane wave generator system for device and life person testing (left). System testing in the factory on a pilot system (right).

II. PWG DESCRIPTION

The millimeter wave PWG is designed according to the guidelines explained in [3-4] as shown in Fig. 2. The array consists of 172 metallic, dual polarized horns, divided in eight subarrays of concentric rings, each excited in equal amplitude and phase by a corporate BFN. The number of sub-arrays and the element density of the PWG are design parameters, linked to the quality of the spherical QZ and the testing distance.

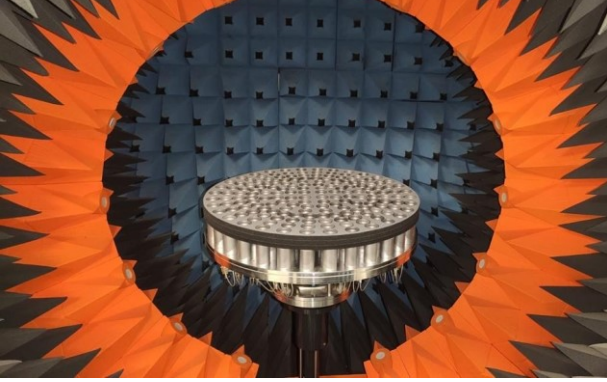


Fig. 2. Testing of the full-size millimeter wave PWG covering the frequency range of 24-30GHz. Testing is performed in the StarLab50GHz spherical near field system of MVG, Paris.

The dual polarized elements of the PWG are circularly symmetric horns. High aperture efficiency is achieved by a shaped smooth walled horn profile, shown in Fig. 3, rather than the traditional assembly of waveguide discontinuities. The design is particularly suited for additive manufacturing using aluminum alloys [8]. The detailed design of the PWG horn is discussed in [9].



Fig. 3. 24-30GHz smooth walled horn element of the PWG array with Euro coin for size comparison (left). Details of the inside and outside of the smooth walled horn from numerical model (right).

The PWG horns are fixed to a printed circuit board (PCB) containing a dual polarized patch antenna as excitation and the corporate BFN for each ring-shaped sub-array. To equalize the phase delay, the path length of each ring is compensated. The PCB multi-layer substrate is a low-loss ceramic laminate with dielectric constant of 3.4. More details of the BFN are discussed in [9].

The relative excitation of the ring-shaped subarrays is digitally controlled and responsible for the quality of the plane wave approximation in the QZ. The sub-array complex weights are frequency dependent, although only minimum variation with frequency is observed in the 24-30GHz range. The optimum coefficients for the PWG are determined experimentally.

The first step in the synthesis of the PWG excitation consists of the evaluation of the radiated field from each ring-shaped sub-array in the QZ volume ($\mathbf{E}_{QZ}(x, y, z)$). Each sub-array is measured individually in a spherical NF system as shown in Fig. 2. The measured field is denoted as $\mathbf{E}_{meas}(r, \phi, \vartheta)$. From each measurements the sub-array radiation is determined at any point inside the QZ by post-processing exploiting the Spherical Wave Expansion (SWE) theory [10] in the following way. The SWE formula shown in Fig. 4 is first inverted to compute the Spherical Wave Coefficients (SWC or $Q_{smn}^{(3)}$) from the measured spherical NF ($\mathbf{E}(\mathbf{r}) = \mathbf{E}_{meas}(r, \phi, \vartheta)$). To do that spherical basis functions ($\mathbf{F}_{smn}^{(3)}(\mathbf{r})$) are evaluated at measurement point locations (r, ϕ, ϑ) [10]. From the computed SWC, the radiated field in the QZ ($\mathbf{E}(\mathbf{r}) = \mathbf{E}_{QZ}(x, y, z)$) is computed using the SWE as forward operator evaluating the basis functions in the wanted locations (x, y, z).

$$\mathbf{E}(\mathbf{r}) = \frac{k}{\sqrt{\eta}} \sum_{s=1}^2 \sum_{n=1}^{\infty} \sum_{m=-n}^n Q_{smn}^{(3)} \mathbf{F}_{smn}^{(3)}(\mathbf{r})$$

Fig. 4. Evaluation of the radiated field in the QZ from each ring-shaped sub-array using NF measurements and the spherical wave expansion formula.

The second step of the synthesis process is schematized in Fig. 5 (for simplicity, and only to illustrate the concept, a simpler PWG device with only four rings is shown in Fig. 5). The different contributions from the sub-arrays are weighted to approximate the plane wave in the QZ. The synthesis domain is represented by a discrete number of points, or stations, fully defining the QZ in 3D space. The excitation synthesis is performed through a non-linear optimization, minimizing an objective function. In this case, the objective function is not limited to the best approximation of a plane wave by minimizing the field deviation, but also to ensure that the total radiated energy is concentrated in the QZ. The advantage of this formulation is to minimize field outside the synthesis domain.

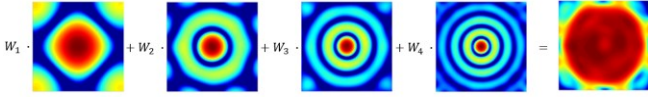


Fig. 5. Conceptual illustration of the QZ synthesis process. Each ring-shaped subarray gives different contribution to the QZ. By optimum weighting of the contributions a plane wave can be approximated.

The PWG can dynamically synthesize different size QZ's up to the maximum size depending on the application. This is due to the digital control and measurement-based optimization procedure. A smaller QZ will have less free space losses due to the gain of the PWG. This can be advantageous in cases where small devices requiring higher S/N ratios are to be measured.

III. PWG DESIGN JUSTIFICATION

To appreciate the advantage of the PWG as a measurement system, it can be compared to direct far field measurements using different probes. The resulting QZ in a volume of 350mm at 1200mm distance, provided by a short electrical dipole, a 15dBi Gaussian probe and the 172 element PWG are compared in Fig. 6. The QZ fields have been determined from numerical simulation including a full-wave model of the PWG. The short electrical dipole is not a practical probe but is included as reference. The values have been normalised for comparison.

The expected downrange amplitude taper caused by the free space attenuation of the dipole and the Gaussian probe is evident in the top-left and centre-left maps of Fig. 6, respectively. Similarly, a strong off-axis phase variation is observed in the top-right and centre-right plots, respectively. The plane wave approximation in the QZ volume of the PWG include a spatially fast varying ripple in amplitude and phase. The expected variation is within $\pm 0.5\text{dB}$ and $\pm 10^\circ$ as can be seen in the bottom-left and bottom-right maps, respectively. The variation is controlled by the PWG excitation. The spatial frequency of the ripple depends on the number of ring-shaped subarrays, their spacing and the overall size of the PWG.

The differences in QZ quality are also evident in the cut through the centre of the QZ illustrated in Fig. 7. If the device under test occupies a significant fraction or the entire QZ of 350mm, only the PWG system can measure the device with a respectable accuracy. This is the case of live person testing or phantom-based tests.

However, in case of measurement scenarios of smaller devices that are centred in the system, both PWG and the FF solutions provide good measurements. In measurement scenarios in which the source of radiation is offset, but occupies a relatively small portion of the QZ and thus subject to less phase variation, the measurements are also acceptable in a FF system. In cases where the exact offset position is known, this knowledge can be used in a post-processing step to clean the direct FF measurement.

For measurement in the PWG system, the knowledge of the exact position of the source of radiation is not necessary. The only requirement is the source to be within the boundaries of the QZ ("black-box" approach).

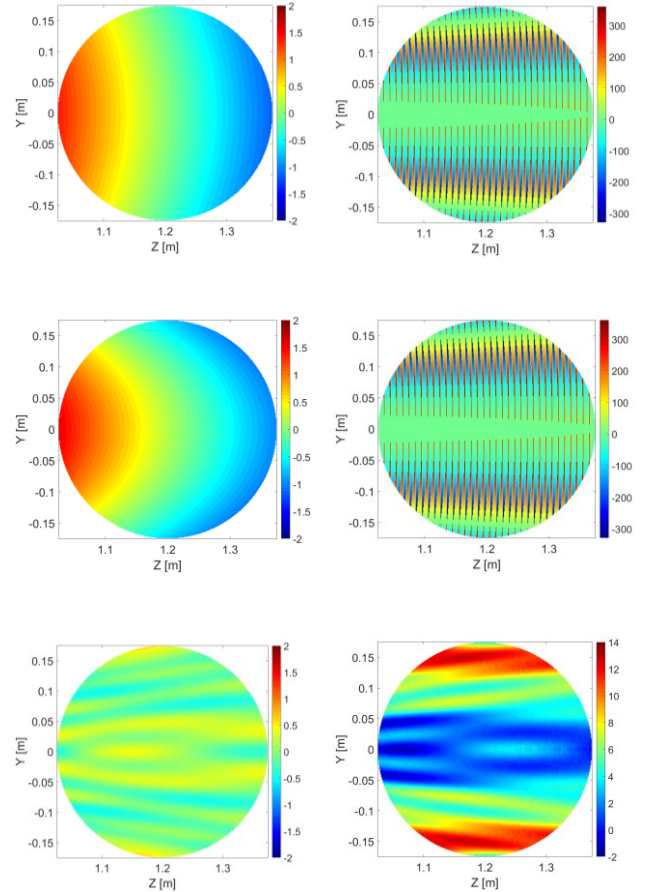


Fig. 6. Amplitude field variation (left) and phase difference wrt an ideal plane wave (right) in the QZ of the different measurements devices at $X = 0\text{ m}$: short electrical dipole (top); 15dBi Gaussian probe (center); PWG (bottom).

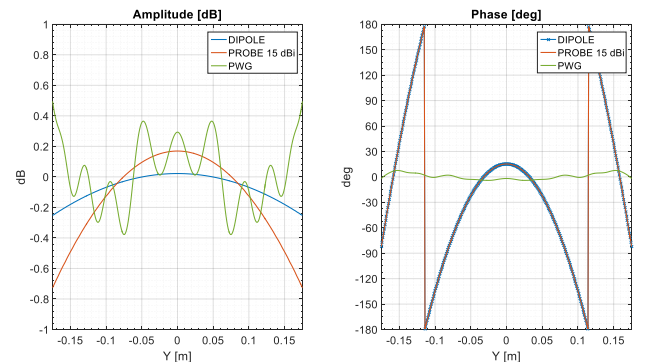


Fig. 7. Normalized amplitude (left) and phase (right) of the field radiated by the different measurements devices at $(X, Z) = (0, 1.2)\text{ m}$.

IV. MEASUREMENT PERFORMANCE EMULATION

An assessment investigation of the performance of the PWG was performed emulating different measurements. The emulated measurement scenario is depicted in Fig. 8.

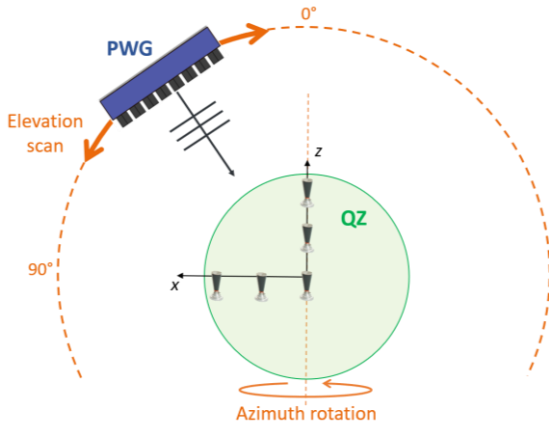


Fig. 8. Emulation of PWG measurement with the QR18000 as DUT in different offset positions along x- and z-axis within the QZ.

A full-wave model of the PWG with 350mm QZ was used in the emulations. A full-wave model [11] of a closed boundary quad-ridge horn, QR18000 [12] at 30 GHz was used for the Device Under Test (DUT). Different DUT positions within the QZ have been considered to mimic realistic DUT with arbitrary source of radiation. Various displacements were considered along the x- and z-axis, while still maintaining the DUT fully within the QZ, as shown in Fig. 8. For comparison, measurement emulations were also performed using the short electrical dipole and the 15dBi gaussian probe for the same scenario and DUT.

Adding further realism to the simulations, a noise floor of -100 dBm, corresponding to the noise floor of typical RF instrumentations, is considered. Moreover, realistic losses of the PWG and both probes are taken into account emulating a plausible signal to noise level of approximately 50-65 dB, depending on the used device. The comparison results are based on gain normalized patterns. The gains have been determined by gain substitution method [2]. The calibration of each system required and additional emulation step considering an ideal Huygens' source as a reference antenna. The measurement emulations are performed by applying the transmission formula described in [10]. The formula gives the coupling between a transmitting DUT and a receiving device, such as the PWG, where the spherical spectrum of both devices is known. The spherical wave spectrum for all devices are computed from the full-wave simulations. The emulated E-plane gain measurements of the QR18000 offset along the x-axis of 90mm is shown in Fig. 9. The black-dotted trace is the reference pattern. The blue and oranges traces are the patterns measured respectively with the dipole and the 15dBi probe. As can be noticed, the offset position of the DUT, combined with the spherical wave fronts of the two probes at the considered measurement distance of 1200mm, causes a non-negligible error in the pointing direction of the pattern. As

expected, the PWG measurement emulations has no pointing error, as illustrated by the green trace.

It can be noted that the measurement emulated with the dipole provides a worse dynamic range resulting in a much noisier pattern. Instead, the gain patterns emulated for both the 15dBi probe and the PWG have higher dynamic range resulting, in turn, in a less noisy measurement. It should be noted that the dynamic range obtained with the PWG in this example can be improved if a smaller QZ are synthesized, as this will increase the effective PWG system gain.

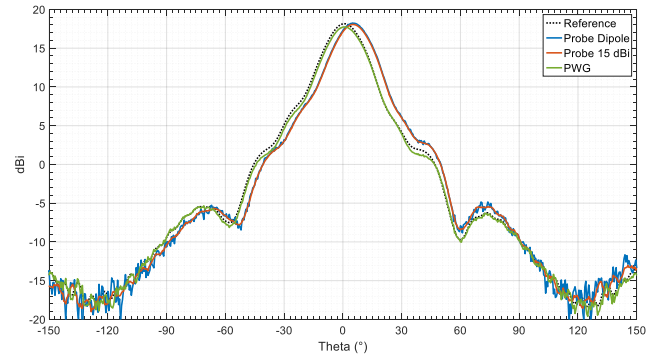


Fig. 9. Measurement emulation - gain pattern comparison of the QR18000 at 30 GHz. The AUT is offset of 90 mm along the x-axis.

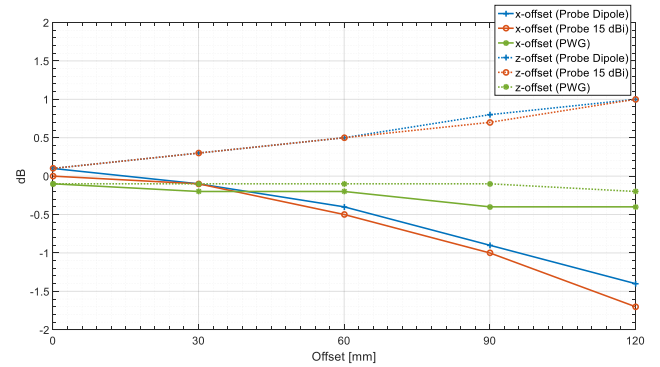


Fig. 10. Measurement emulation of PWG and direct FF measurement with dipole or Gaussian probe as range antenna. Comparison of boresight gain error with offset distance in X or Z direction.

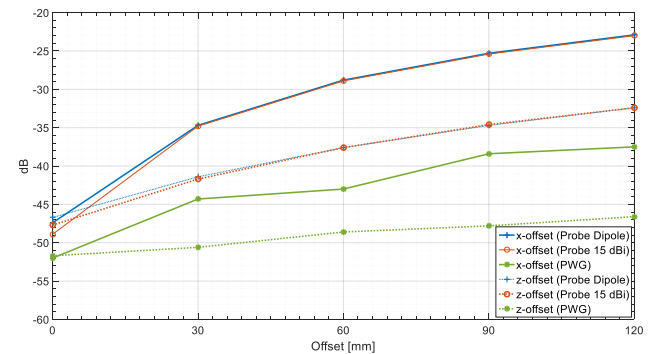


Fig. 11. Measurement emulation of PWG and direct FF measurement with dipole or Gaussian probe as range antenna. Comparison of the Equivalent Noise Level (ENL).

Boresight gain error for the different measurement scenarios can also be evaluated using the measurement emulation technique. The gain error is computed for each offset of the DUT and for each of the three measurement devices as shown in Fig. 10. The systems are presumed to be gain calibrated with the reference antenna in the centered position. As expected, boresight gain error increases dramatically in both FF systems when the dipole or the 15dBi element are used as probes. An offset along the x-axis is more critical and the gain error reaches a value of 1.7 dB. On the contrary, the PWG gives virtually the same result in any position within the QZ. The highest observed gain variation with offset is in fact 0.4 dB.

The global pattern accuracy in the different scenarios can be estimated with the Equivalent Noise Level (ENL) defined by the following formula:

$$ENL = 20 \log_{10} \left(RMSE \left| \frac{E(\theta, \varphi) - \tilde{E}(\theta, \varphi)}{E(\theta, \varphi)_{MAX}} \right| \right)$$

where $E(\theta, \varphi)$ is the reference and $\tilde{E}(\theta, \varphi)$ is the test pattern. The ENL comparison is reported in Fig. 11. As expected, the increase in error levels with DUT offset is confirmed for direct FF systems with dipole or 15dBi element as probes or range antennas. The corresponding error levels are up to 15 dB better with the PWG.

V. PILOT SYSTEM MEASUREMENTS

The closed boundary quad-ridge horn QR18000 has been measured in the pilot system as a factory test. The testing scenario is shown in Fig. 1. The test was performed in non-anechoic conditions to verify the quality of the PWG QZ. The DUT was measured in three position at 27.5GHz, with the same orientation but offset 0cm, -8cm and 11cm in the Z direction. This is an effective reduction in PWG to DUT distance as shown in Fig. 8. The measured patterns are shown in Fig. 12 and compared to full wave simulation.

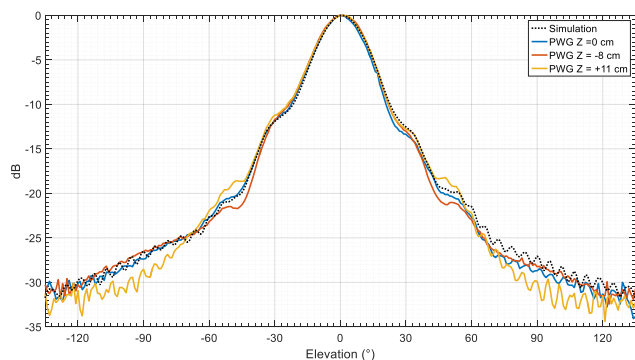


Fig. 12. Comparison between full-wave simulation and PWG measurements of the QR18000 quad-ridge horn at 27.5 GHz performed with different offset distance along the z-axis.

The measurements and simulations are in very good agreement. Some variations between the offset patterns and the on-set measurement and simulation can be noticed at

elevation 45° from boresight around the -20dB pattern levels. This is believed to be a consequence of the non-anechoic testing conditions in the factory.

Further measurements on the final PWG testing system will be presented during the presentation of this paper.

VI. CONCLUSION

The measurement performance and system level accuracy of a recently developed plane wave generator (PWG) at millimeter wave frequencies has been discussed. This full-size PWG consist of 172 dual polarized elements divided in eight-rings. The array excitation is regulated by a combination of corporate BFN and digital control. The PWG is integrated in an automated system for full 3D device measurements.

Simulations of measurement scenarios demonstrate the advantage of a full-size quiet zone (QZ) in limited space and gives indications on the expected performances of the system. Preliminary measurements in the factory on a pilot system, on a medium gain horn in different positions in the QZ confirm the expected performance of the system. Testing results, demonstrating the final system should be available for the presentation of this paper.

REFERENCES

- [1] "IEEE Standard Test Procedures for Antennas," ANSI/IEEE Std 149-1979.
- [2] "IEEE Recommended Practice for Near-Field Antenna Measurements" IEEE std 1720-2012.
- [3] F. Scattoni, D. Sekuljica, A. Giacomini, F. Saccardi, A. Scannavini, L. J. Foged, E. Kaverine, N. Gross, P. O. Iversen, "OTA Testing of Antennas & Devices using Plane Wave Generator or Synthesizer", 14th European Conference on Antennas and Propagation, EuCAP 2020.
- [4] F. Scattoni, D. Sekuljica, A. Giacomini, F. Saccardi, A. Scannavini, P. O Iversen, E. Kaverine, N. Gross, L. J. Foged "Comparative Testing of Devices in a Spherical Near Field System and Plane Wave Generator", AMTA 2019
- [5] Y. Zhang, Z. Wang, X. Sun, Z. Qiao, W. Fan and J. Miao, "Design and Implementation of a Wideband Dual-Polarized Plane Wave Generator With Tapered Feeding Nonuniform Array," in IEEE Antennas and Wireless Propagation Letters, vol. 19, no. 11, pp. 1988-1992, Nov. 2020
- [6] S. Catteau, M. Ivashina and R. Rehammar, "Design and Simulation of a 28 GHz Plane Wave Generator for NR Measurements," EuCAP 2020, Copenhagen, Denmark
- [7] <https://www.youtube.com/watch?v=SUccig3vSlS&feature=youtu.be>
- [8] L. J. Foged et al., "Investigation of Additive Manufacturing for Broadband Choked Horns at X/Ku Band," in IEEE Antennas and Wireless Propagation Letters, vol. 17, no. 11, pp. 2003-2007, Nov. 2018.
- [9] F. Scattoni, D. Sekuljica, A. Giacomini, F. Saccardi, A. Scannavini, S. Anwar, N. Gross, E. Kaverine, P. O Iversen, L. J. Foged, "Towards testing of 5G millimetre wave devices using plane wave generators", 15th European Conference on Antennas and Propagation, EuCAP 2021, Dusseldorf, Germany
- [10] J. E. Hansen (ed.), "Spherical Near-Field Antenna Measurements", Peter Peregrinus Ltd., London, United Kingdom, 1988
- [11] <https://www.3ds.com/products-services/simulia/>
- [12] <https://www.mvg-world.com/en/products/antennas/measurement-probes-and-feeds/closed-boundary-quad-ridge-horns>